Available online at www.sciencedirect.com
SCIENCE DIRECT®
Materials Science and Engineering C 26 (2006) 1146 – 1150
MATERIALS SCIENCE & ENGINEERING C
www.elsevier.com/locate/msec

Epitaxial growth of Fe nanodots on SrF_2/Si (111)

H. Hosoya *, M. Arita, K. Hamada, Y. Takahashi

Graduate School of Information Science and Technology, Hokkaido University, Kita-14, Nishi-9, Kita-ku, Sapporo 060-0814, Japan

Available online 21 November 2005

Abstract

Fe nanodots were grown on SrF_2 (111) surfaces deposited on Si (111) substrates in a molecular beam epitaxy (MBE) system. The crystallographic and surface morphological characters were studied by reflection high-energy electron diffractometry (RHEED) and atomic force microscopy (AFM). The triangular terraces and step edges of SrF_2 were formed at 600 °C, and its crystallinity was high in quality. Fe (111) layers with thicknesses between 0.5 and 5 nm were grown epitaxially on this SrF_2 layer at room temperature (RT) with the help of electron beam exposure. In 1-nm thick Fe layers deposited at RT, the number density was about 2×10^{12} cm^{-2}. At the end of this report, an epitaxial growth of the SrF_2/Fe/SrF_2 tri-layer on Si (111) is briefly described.

Keywords: Fe nanodot; Epitaxial growth; SrF_2; Si (111) surface

1. Introduction

In the last decade, semiconductor nanostructures have been vigorously investigated for the physics and engineering of single electron tunneling (SET) effects such as the Coulomb blockade (CB) and the Coulomb staircase (CS) phenomena [1]. Meanwhile, in the field of magnetic devices, ferromagnetic thin films and multilayers have attracted considerable attention for usage of spin-dependent transport effects such as tunneling magnetoresistance (TMR) [2]. Fusion of these two effects, SET and TMR, is expected to generate a hybrid spintronic device [3]. Ferromagnetic nanodot systems such as Fe–MgO granular films, where dots are dispersed in an insulator matrix, are candidates for study in this research field. The nanoscale conductive characteristics of magnetic nanodots have been intensively studied in recent years [4–8], and the enhancement and the oscillation of TMR have been reported.

Randomness of size and dispersion of nanodots in granular films may lead to a widely distributed charging energy. Therefore, to use quantum effects (i.e., CB and CS), homogeneous arrangement of nanodots is needed. Ernult et al. reported a fabrication of self-assembled Fe dots epitaxially grown on MgO (001) [8,9]. Iron possesses high surface energy, so an island growth is expected. They found that epitaxial growth is effective in accomplishing homogeneous dot size. While the results obtained in the reports mentioned above are useful, another key factor remains necessary for developing spintronic devices made of nanodots. This is a usage of Si substrates, since Si technology will be needed to fabricate actual devices.

We therefore investigated the possibility of fabricating epitaxially grown Fe nanodots on insulator/Si substrates. Strontium fluoride (SrF_2) was selected as the insulator, which is known to grow epitaxially on Si (111) surfaces [10,11] and has a fluorite (CaF_2) structure. In addition, the lattice parameter of cubic SrF_2 (a_{SrF2}) is 0.580 nm, double of that of bcc-Fe (a_{Fe}=0.287 nm). The mismatch of a_{SrF2} and a_{Fe} is approximately 1%. In the following section, experimental factors to grow bcc-Fe nanodots epitaxially on SrF_2/Si (111) will be described.

2. Experimental

A molecular beam epitaxy (MBE) system (base pressure: $<6 \times 10^{-9}$ Pa) was used to grow Fe nanodots and SrF_2 layers. First, a few-nanometer thick Si oxide layer was formed on a Si (111) substrate by a chemical treatment using a mixture of H_2O_2 and H_2SO_4. Next, the surface SiO_2 was sublimated in the MBE system by a heat treatment at 800 °C for 1 h. Here, we confirmed a 7×7 clean surface by reflection high-energy electron diffractometry (RHEED).

* Corresponding author. Tel.: +81 11 706 6457.
E-mail address: hosoya@nano.ist.hokudai.ac.jp (H. Hosoya).

0928-4931/$ - see front matter © 2005 Elsevier B.V. All rights reserved.
doi:10.1016/j.msec.2005.09.051

The deposition was performed in the MBE chamber by electron beam evaporation of two solid sources: metallic Fe ingot (99.95%) and sintered SrF_2 tablet (99.9%). The vacuum during the deposition was better than 6×10^{-7} Pa. The typical deposition rate was 0.01 nm/s for both materials. Three types of film structures were fabricated: SrF_2/Si, Fe/SrF_2/Si, and SrF_2/Fe/SrF_2/Si. Deposition temperatures (T_s) between 600 °C and room temperature (RT) were tested. Some films deposited at RT were annealed at 300 °C for 1 h in order to increase the crystallinity. The details about T_s and thickness will be described in the next section. The structures of the films were observed by in situ or ex situ RHEED operated at 20 kV. The surface morphology of the films was investigated by atomic force microscopy (AFM) in air.

3. Results and discussion

3.1. SrF_2/Si (111)

First, epitaxial growth of SrF_2 on Si (111) was confirmed. The layer thickness of SrF_2 was 20 nm. The data of SrF_2 deposited at 600 °C are presented in Fig. 1a–c. The RHEED pattern (Fig. 1a) shows sharp streaks with Kikuchi lines. This indicates that the crystal is highly qualified. Comparing this pattern with that of Si predicts a relation (111)<110>$_{SrF2}$// (111)<110>$_{Si}$. Triangular terraces and steps can be seen in the AFM image (Fig. 1b). The step edge direction is <110>. A similar structure was reported in the CaF_2/Si (111) system [12]. Two types of stacking layers appeared in the SrF_2/Si system. One of them had the same orientation as the substrate, and the other was rotated by 180°. Trenches such as a black contrast in this figure are due to the different stacking layers. The height profile along the dashed line in Fig. 1b is presented as Fig. 1c. The minimum distance between step edges was about 20 nm and the step height was approximately 0.35 nm, which corresponds to (111) lattice spacing. While the local region on the terrace was almost atomically flat, the overall area was rather rough. The R_a value in Fig. 1b is 0.78 nm.

Fig. 1d–f are the data obtained from SrF_2 prepared at RT followed by annealing at 300 °C for 1 h. The RHEED pattern (Fig. 1d) was quite similar to that obtained by depositing SrF_2 at 600 °C (Fig. 1a), although no Kikuchi lines appeared. The crystallinity in this case was lower than that of Fig. 1a, although it is thought to be sufficient. According to the AFM

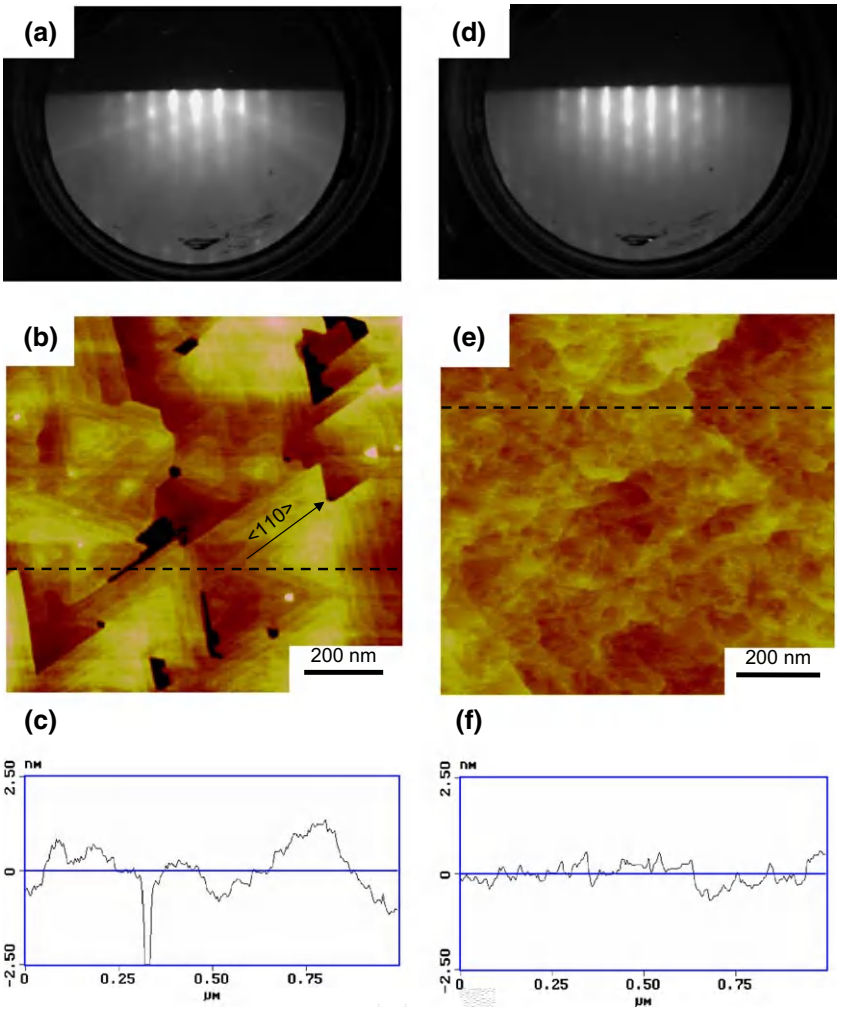

Fig. 1. RHEED patterns (azimuth: <110>) and AFM images of SrF_2 layer deposited at (a)–(c) 600 °C and (d)–(f) RT (with anneal at 300 °C for 1 h). (c) and (f) Height profiles along dashed lines in AFM images (b) and (e).

image, specific step and terrace structures were not formed, and no clear trench was formed (Fig. 1e). A height profile along the dashed line in Fig. 1e is shown in Fig. 1f. The overall profile is smoother than that obtained at 600 °C (Fig. 1c), as the R_a value is 0.3 nm. The SrF_2 layer at RT seems better for fabricating test devices than that at 600 °C. However, considering only the surface in the local area, the deposition at 600 °C provided a better structure. In the following, therefore, the SrF_2 layer prepared at 600 °C was mainly used for epitaxy tests.

3.2. Fe/SrF_2/Si (111)

On the deposited SrF_2 (111) layers, Fe layers composed of nanodots were prepared. Fig. 2a is a RHEED pattern observed after deposition of 1-nm thick Fe at T_s=RT. The pattern is halo-like and no trace of epitaxy is recognized. However, by the electron beam irradiation for the ex situ RHEED observation, the pattern became spotty (Fig. 2b). This result may indicate that the crystallinity increased and/or that clear Fe dots were formed during the beam irradiation. This pattern shows the (111) epitaxy of Fe while some (110) growth is recognized. To clarify the influence of the electron beam, the Fe layer was deposited with an electron beam exposure by in situ RHEED (Fig. 2c). In this pattern, the (111) epitaxial growth is more clearly visible. The pattern is rather spotty and the orientation relation is (111)<110>$_{Fe}$// (111)<110>$_{SrF2}$. This phenomenon was recognized for both the SrF_2 (111) layer deposited at 600 °C and that deposited at RT. The Fe layer grew epitaxially up to 5 nm in thickness. In thicker films, a ring pattern appeared.

Two factors were considered to clarify the role of electron beam for the epitaxial growth: temperature increase by the beam and direct interaction between the material and the beam. To check the influence of temperature, Fe was deposited at 300 °C (Fig. 2d). In this RHEED pattern, 110_{Fe} and 112_{Fe} spots show clearly, indicating intrinsic (110) growth. The streak pattern from SrF_2 is clearly visible in this figure. This indicates that Fe particles grew large and that the distance between particles spread out. The temperature increment did not yield (111) epitaxy. Relating to the interaction between the material and the electron beam, there have been some reports about GaAs/CaF_2 (111) [13–15]. These reports have established that the fluorine-terminated (111) surface of CaF_2 is energetically stable and inactive, and that the uppermost fluorine atoms are desorbed by the electron beam. As a result, strong As–Ca bonds are formed and the epitaxy of GaAs on CaF_2 improves. A similar result is expected for SrF_2, which has the same crystal structure and similar chemical nature as CaF_2.

The surface morphologies of the Fe dot layers deposited at RT are presented in Fig. 3a and b. The Fe thicknesses are 0.5 and 1.0 nm, respectively. The AFM images confirm the 3D growth of Fe layers in a uniform distribution. The typical dot diameter estimated from these images is approximately 8–10 nm. Because the AFM image corresponds to the surface morphology convoluted by the tip shape (apex size: larger than 10 nm) [16], the net dot size is thought to be much smaller than this value, probably several nanometers smaller than the estimated size. The number density of the Fe dots was 2.0×10^{12} and 2.3×10^{12} cm^{-2} for Fig. 3a and b, respectively. These values correspond well to those of the dot film prepared on MgO [9]. By increasing the substrate temperature for Fe deposition, the dot size increased to 15 nm and the number density was significantly reduced (Fig. 3c). The dot formation was at the step edges. This corresponds to the RHEED pattern shown in Fig. 2d and is a very usual crystal growth. Table 1 summarizes these results.

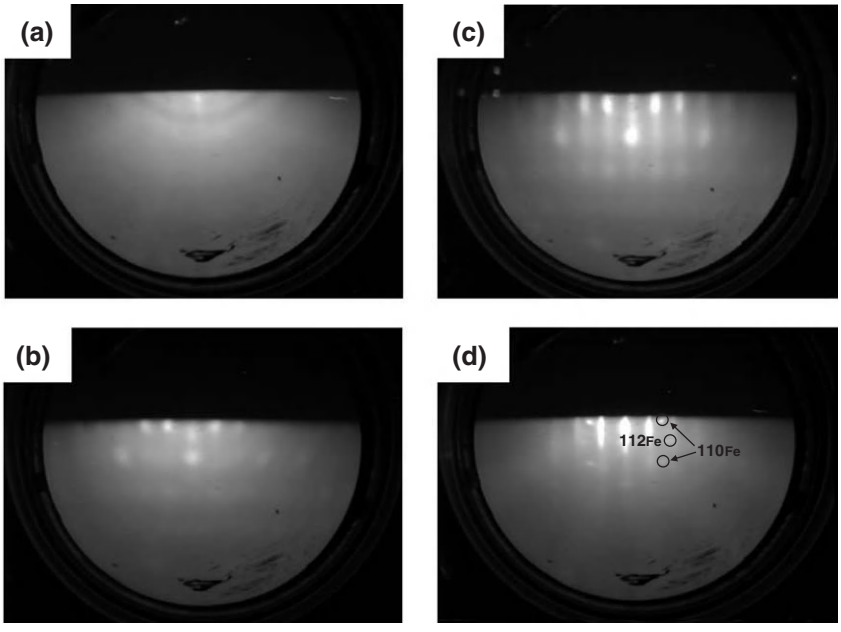

Fig. 2. RHEED patterns (azimuth: <110>) of Fe layers (1-nm thick) deposited on SrF_2 (111) shown in Fig. 1b. (a) A layer prepared at RT, (b) the layer shown in Fig. 2a after a long ex situ electron beam exposure, (c) a layer deposited at RT with an in situ electron beam exposure, and (d) a layer deposited at 300 °C.

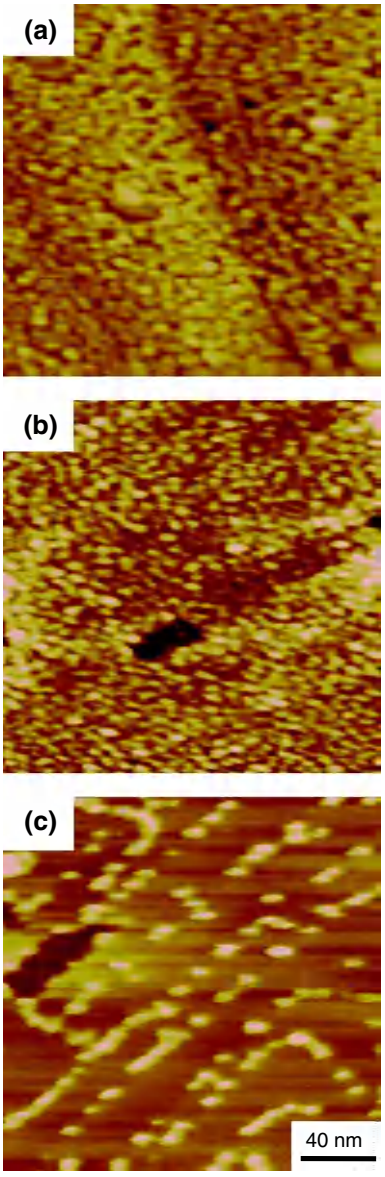

Fig. 3. AFM images of Fe layers on SrF_2 (111) prepared at 600 °C with no electron beam exposure. Substrate temperatures and the thickness are (a) RT and 0.5 nm, (b) RT and 1.0 nm, and (c) 300 °C and 1.0 nm.

3.3. SrF_2/Fe/SrF_2/Si (111)

Next, a 1-nm thick SrF_2 layer was deposited at RT on the film shown in Fig. 2b. The RHEED patterns during the series of depositions are shown in Fig. 4. The spotty pattern from the Fe nanodot layer recovered streaky by deposition of the SrF_2 thin layer. The same thing was accomplished for SrF_2 deposition on the film in Fig. 2d with no (111) epitaxy. Epitaxial growth of the SrF_2 top layer is probably due to the SrF_2 bottom layer being partly exposed to the film surface. A tri-layer film where Fe dots are sandwiched by two SrF_2 layers was expected to be formed by this procedure, regardless of the Fe epitaxy.

Table 1
Density of Fe dot and epitaxy grown at RT and 300 °C on SrF_2 (111) layer deposited at 600 °C

Growth temperature of Fe	Film thickness (nm)	Density of dots (cm^{-2})	(111) orientation
RT	0.5	2.0×10^{12}	○
RT	1.0	2.3×10^{12}	○
300 °C	1.0	3.2×10^{11}	×

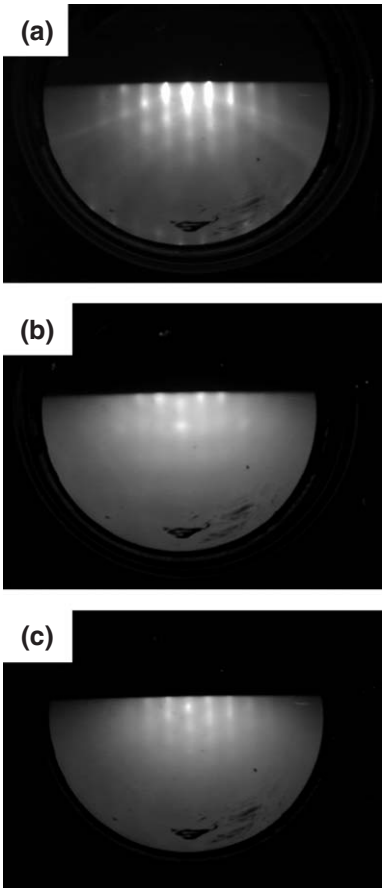

Fig. 4. RHEED patterns of a SrF_2/Fe dot/SrF_2 tri-layer film on Si (111) for the azimuth <110>. (a) SrF_2 bottom layer (20-nm thick, 600 °C) on Si, (b) Fe layer (0.5-nm thick, RT) with ex situ beam exposure, and (c) SrF_2 top layer (1-nm thick, RT).

4. Conclusion

The epitaxial growth of Fe nanodots was investigated on SrF_2 (111) surfaces prepared on Si (111). At substrate temperatures of RT and 600 °C, SrF_2 (111) layers were obtained with relatively smooth surfaces. The nanodots of Fe were epitaxially grown at RT with the help of electron beam exposure. Considering earlier reports on CaF_2 [13–15], the electron beam is thought to desorb fluorine atoms from the SrF_2 (111) surface and to enhance the bond strength between Sr and Fe. By SrF_2 deposition on thin film, a tri-layer film composed of a Fe (111) nanodot layer sandwiched by two SrF_2 (111) layers was fabricated. Although further optimization of growth conditions should be explored to fabricate films without pin-holes that generate a current leakage path, the results of the present study are an important step in developing spin-dependent SET devices formed on Si substrates.

Acknowledgements

We are grateful to Professor M. Yamamoto for permission to use the AFM instrument at Hokkaido University. This work was supported by the Murata Science Foundation, the Izumi Science and Technology Foundation, and a grant-in-aid from the Japan Society for the Promotion of Science (Nos. 13650708, 16206038, and 17201029).

References

[1] Y. Takahashi, Y. Ono, A. Fujiwara, H. Inokawa, J. Phys. Condens. Matter. 14 (2002) 995 (related references therein).
[2] E. Hirota, H. Sakakima, K. Inomata, Giant Magneto-Resistance Devices, Springer, Berlin, 2002, related references therein.
[3] K. Ono, H. Shimada, Y. Ootuka, J. Phys. Soc. Jpn. 66 (1997) 1261.
[4] L.F. Schelp, A. Fert, F. Fettar, P. Holody, S.F. Lee, J.L. Maurice, F. Pertoff, A. Vaures, Phys. Rev., B. 56 (1997) 5416.
[5] C.T. Black, C.B. Murray, R.L. Sandstorm, S. Sun, Science 290 (2000) 1131.
[6] S. Takahashi, S. Maekawa, Phys. Rev. Lett. 80 (1998) 1758.
[7] K. Nakajima, Y. Saito, S. Nakamura, K. Inomata, IEEE Trans. Magn. 36 (2000) 2806.
[8] F. Ernult, K. Yamane, S. Mitani, K. Yakushiji, K. Takanashi, Y.K. Takanashi, K. Hono, Appl. Phys. Lett. 84 (2004) 3106.
[9] F. Ernult, S. Mitani, Y. Nagano, K. Takanashi, Sci. Technol. Adv. Mater. 4 (2003) 383.
[10] T. Asano, H. Ishiwara, N. Kaifu, Jpn. J. Appl. Phys. 22 (1983) 1474.
[11] M.A. Olmstead, R.D. Bringans, J. Electron Spectrosc. Rel. Phenom. 51 (1990) 599.
[12] C.R. Wang, B.H. Muller, K.R. Hofmann, Thin Solid Films 410 (2002) 72.
[13] K. Saiki, Y. Sato, K. Ando, A. Koma, Surf. Sci. 192 (1987) 1.
[14] H.J. Ko, Y.F. Chen, J.M. Ko, T. Hanada, Z. Zhu, T. Fukuda, T. Yao, J. Cryst. Growth 207 (1999) 87.
[15] H.C. Lee, T. Asano, H. Ishiwara, S. Furukawa, Jpn. J. Appl. Phys. 27 (1988) 1616.
[16] M. Nagase, H. Namatsu, K. Kurihara, K. Iwadate, K. Murase, Jpn. J. Appl. Phys. 34 (1995) 3382.